Analysis on the Interactions of Harmonics in Exhaust Pipes of Automotive Engines

Min-Ho Lee

Graduate School of Mechanical Engineering, Myong-Ji University, 449-728, Korea

Joon-Seo Lee

Department of Mechanical Design, Chung-Cheong College, 363-890, Korea

Kyung-Ok Cha*

Department of Mechanical Engineering, Myong-Ji University,
San 38-2 Nam-dong, Yong-in city, Kyunggi-do, 449-728, Korea

In exhaust pipes of automotive engines, the pulsating pressure waves are composed of fundamental frequency and high order harmonics. The nonlinearities in the exhaust pipe is caused by their interactions. The error between prediction and measurement is induced by the nonlinearities. We can not explain this phenomenon using linear acoustics theory. So power spectrum, which is used in linear theory, is not useful. This paper is concerned with the development of useful engineering techniques to detect and analyze nonlinearity in exhaust pipe of automotive engines. The study of higher order statistics has been dominated by work on the bispectrum. The bispectrum can be viewed as a decomposition of the third moment (skewness) of a signal over frequency and as such is blind to symmetric nonlinearities. The phenomenon of quadratic phase coupling (QPC) can be analyzed by the bicoherence function. Finally the application of these techniques to data from actual exhaust pipe systems is performed.

Key Words : Pulsating Pressure Waves, Higher Order Statistics, Bispectrum, Quadratic Phase Coupling (QPC), Bicoherence

1. Introduction

Intake and exhaust noises from internal combustion engines are a major contributor to a noisy evironment affecting millions of people. Exhaust noise levels are often near, or even exceed, 90 dBA at the operator's location. Because of its low-frequency content, exhaust noise propagates with little attenuation into people's homes, recreational areas, and work places.

When only acoustics are of concern, mufflers may be readily designed to achieve virtually any

----

* Corresponding Author,
  E-mail : chako@mju.ac.kr
  TEL : +82-31-330-6420; **FAX** : +82-31-321-4959
  Department of Mechanical Engineering, Myong-Ji University, San 38-2 Nam-dong, Yong-in city, Kyunggi-do, 449-728, Korea. (Manuscript **Received** August 16, 2003; **Revised** October 6, 2003)

level of control of intake or exhaust noise (Davis, 1964). Generally, increasing levels of attenuation may be reached with increasing muffler volume, weight, and back-pressure (at the engine manifold). However, all of these parameters adversely affect the cost and performance of the vehicles to which mufflers are applied. For examples, the back-pressure of an exhaust system may degrade engine performance by a few percent (Eizo Suyama and Takashi Ishida, 1990).

The noise radiated from out internal combustion engine and propagated through the exhaust gas medium is statistically analyzed and characterized as a stochastic process deriving from the combination of different components. The radiated noise is expected to be produced by periodical, almost periodical and non linear processes. For the reason its complete statistical characterization needs non conventional spectral analysis. Con-

ventional digital signal processing is based on Fourier theory. By means of Fourier analysis, only linear mechanisms can be studied, since supposed uncorrelation among harmonic components implies phase information suppression. Power spectrum (Seybert and Hamilton, 1978 ; Lyon, 1975 ; Bendat and Piersol, 1993) information is not sufficient in case of non-Gaussianity and non-linearity.

In the present paper Higher order spectra techniques (Bispectrum analysis) (Nikias and Mendel, 1993 ; Nikias and Petropula, 1993 ; Nikias and Raghuveer, 1987 ; Miksad et al., 1983) for analysis and detection purposes are employed, in comparison with the conventional Fourier approach. Higher order spectral theory has been preferred since it is a useful thing to cover a lot of nonlinear fields and is suitable for general signal processing.

2. Higher Order Spectral Theory

2.1 Expectation, probability density functions and moments

Given any signal $g(x)$, the expected value of $g(x)$ is defined as

$$E[g(x)] = \int_{-\infty}^{\infty} g(x)\, p(x)\, dx \qquad (1)$$

where, E is the expectation operator. Also, the expected value of $g(x)$ is the average of $g(x)$ weighted by the likelihood of x occurring, as given by the probability density function of x.

The moments of a stationary random process $\{x(t)\}$ representing a physical phenomenon are defined as

$$u_k = E[x^k] = \int_{-\infty}^{\infty} x^k p(x)\, dx, \ k=0, 1, 2, \cdots \quad (2)$$

where, $p(x)$ is probability density function of $\{x(t)\}$ and μ_k is called the kth moment. For the zero moment $(k=0)$, it is clear that

$$\mu_0 = E[x^0] = \int_{-\infty}^{\infty} x^0 p(x)\, dx = 1 \qquad (3)$$

The first moment $(k=1)$ yields

$$\mu_1 = E[x^1] = \int_{-\infty}^{\infty} x p(x)\, dx = \mu \qquad (4)$$

which is called the mean value of $\{x(t)\}$.

The second moment $(k=2)$ gives

$$\mu_2 = E[x^2] = \int_{-\infty}^{\infty} x^2 p(x)\, dx = \Psi^2 \qquad (5)$$

which is called the mean square value of $\{x(t)\}$ and the positive square root of the mean square value is called the root-mean-square or rms value.

For second and higher moments, it is often convenient to calculate moments about the mean, referred to as central moments. The second central moment is given by

$$\mu^c_2 = E[(x-\mu)^2] = \int_{-\infty}^{\infty} (x-\mu)^2 p(x)\, dx = \sigma^2 \ (6)$$

which is called the variance of $\{x(t)\}$ and the positive square root of the variance is called the standard deviation. The calculation of moment using equation (2) can be extended to as high an order of r as desired.

If x is a stationary, random, signal, the rth moment of $x(t)$, denoted μ_r, is defined as

$$\mu_r = E[x^r(t)] \qquad (7)$$

Note that $\mu_1 = E[x(t)] = \mu_x$, the mean of $x(t)$.

High order moments (Mood et al., 1974) are usually calculated as central moments about the mean. That is

$$\mu_r = E[(x(t) - \mu_x)^r] \qquad (8)$$

The second central moment is the variance of a signal,

$$var[x(t)] = \mu_2 = E[(x(t) - \mu_x)^2] = \sigma_x^2 \quad (9)$$

This gives a measure of the spread of a signal about the mean. The probability density function of a signal with a Gaussian or normal distribution (see Figure 1) is completely described by its mean and variance. Higher order moments are often used to describe the properties of more complex signals. The third moment about the mean, μ_3, is sometimes called skewness and is a measure of asymmetry of the probability density function.

A probability density function similar to that shown by the solid line in Figure 2 is said to be skewed the left and has a negative skewness, while one similar to that shown by the dotted line is
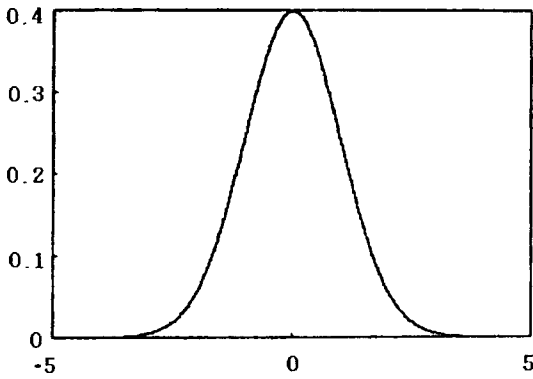
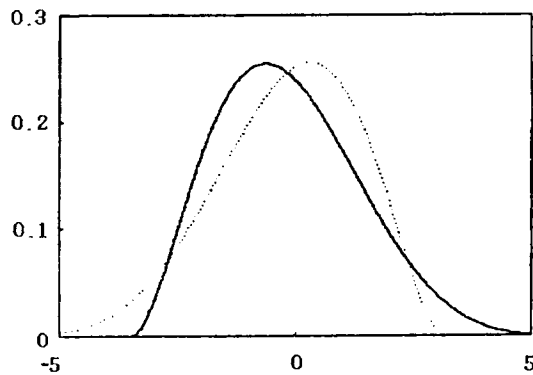**Fig. 1** Gaussian probability density function ($\mu_3=0$, $\mu_4=3$)

Fig. 2 Negative skewed probability density function, (solid line), and positive skewed probability density function, (dotted line)

said to be skewed to the right and has a positive skewness. The ratio μ_3/σ_x^3, which is dimensionless, is called the coefficient of skewness and gives a measure of the degree to which a distribution is skewed.

2.2 Higher order spectrum

The power spectrum and bispectrum are just particular examples of the generalized concept of poly-spectra. Just as the power spectrum is able to give a decomposition of power over frequency, it is possible to use higher order spectra to obtain a decomposition of skewness over frequency and so obtain more information about the higher order statistics of a signal (Priestley, 1981). The power spectrum is the main tool of signal analysis and a huge body of literature has been published

concerning its use and properties. It is the most commonly used of the poly-spectra for being of the lowest order, it is the simplest to calculate and easiest to interpret. The power spectrum is concerned with the second order statistics of a signal and will now be defined both in the context of deterministic and stochastic processes. The energy in signal is

$$\overline{x^2(t)} = \int_{-\infty}^{\infty} x^2(t)\, dt \qquad (10)$$

Substituting $x(t) = \int_{-\infty}^{\infty} X(f)\, e^{j2\pi\pi t}\, dt$ into equation (10) gives,

$$\overline{x^2(t)} = \iiint_{-\infty}^{\infty} X(f_1)\, X(f_2)\, e^{j2\pi t(f_1+f_2)}\, dt\, df_1\, df_2 \qquad (11)$$

Integrating equation (11) with respect to t and using the shifting property of the δ function results in,

$$\overline{x^2(t)} = \iint_{-\infty}^{\infty} X(f_1)\, X(f_2)\, \delta(f_1+f_2)\, df_1\, df_2$$
$$= \int_{-\infty}^{\infty} X(f_1)\, X(-f_1)\, df_1 \qquad (12)$$

From this the energy spectrum can be defined as,

$$E_{xx}(f) = X(f)\, X(-f) \qquad (13)$$

For a stationary stochastic process it is possible to use a similar method, to obtain the power spectrum which is defined as

$$S_{xx}(f_1,\ f_2) = E[X(f_1)\, X(-f_2)] \qquad (14)$$

For a stationary process it can be shown that $S_{xx}(f_1,\ f_2)$ is equal to zero except along $f_1 = -f_2$. This results in the following, more usual, definition for the power spectrum of a stochastics process

$$S_{xx}(f) = E[X(f)\, X^*(f)] \qquad (15)$$

where '*' denotes the complex conjugate. The power spectrum treats each frequency component as independent from all others and measures the power of the signal at each frequency. It is a real quantity and contains no phase information and as such is said to be phase blind. Rather than decomposing the energy of a signal to produce the energy spectrum, it is possible to conduct similar analysis on a cubed signal,

$$\overline{x^3(t)} = \int_{-\infty}^{\infty} x^3(t)\, dt \qquad (16)$$

Substituting $x(t) = \int_{-\infty}^{\infty} X(f) e^{j2\pi ft} df$ into equation (16) gives,

$$\overline{x^3(t)} = \iiiint_{-\infty}^{\infty} X(f_1) X(f_2) X(f_3) e^{j2\pi t(f_1+f_2-f_3)} dt df_1 df_2 df_3$$

$$= \iiint_{-\infty}^{\infty} X(f_1) X(f_2) X(f_3) \delta(f_1+f_2+f_3) df_1 df_2 df_3 \quad (17)$$

$$= \iint_{-\infty}^{\infty} X(f_1) X(f_2) x(-f_1-f_2) df_1 df_2$$

From this, the bispectrum of a deterministic signal can be defined as,

$$E_{xxx}(f_1, f_2) = X(f_1) X(f_2) X(-f_1-f_2) \quad (18)$$

For a stochastic process, using the same method as for the power spectrum, the bispectrum is defined as

$$S_{xxx}(f_1, f_2, f_3) = E[X(f_1) X(f_2) X(f_3)] \quad (19)$$

If the process is stationary, it has been that S_{xxx} (f_1, f_2, f_3) is equal to zero except on the plane $f_3 = -f_1-f_2$. Therefore, the bispectrum of a stationary stochastic process is defined as

$$S_{xxx}(f_1, f_2) = E[X(f_1) X(f_2) X^*(f_1+f_2)] \quad (20)$$

In the same way that the power spectrum is concerned with the power of a signal, or second order moment, the bispectrum is concerned with the skewness, or third order moment. The bispectrum is a function of two frequency variables, f_1 and f_2 and while the power spectrum considers each frequency component independently, the bispectrum analyses the frequency interactions between the components f_1, f_2 and f_1+f_2. It is a complex quantity containing both real and imaginary parts. However, throughout this work only the magnitude of the bispectrum is considered. Two simple examples, using sine waves, are now given demonstrating some of the possible frequency interactions that can occur in the bispectrum. Sine waves are used as an example because they produce easily understood results despite the fact that they do not conform to assumption of being stationary random signals. Consider a complex sine wave of frequency p_1. A complex sine wave is used in order to suppress unwanted cross terms between the positive and negative frequency components.

$$x(t) = e^{j2\pi p_1 t} \quad (21)$$

This has a Fourier transform,

$$X(f) = \delta(f - p_1) \quad (22)$$

where δ represents the Dirac delta function. This is shown diagrammatically in Figure 3. If $X(f)$ is substituted from equation (22) into equation (18), the bispectrum is equal t

$$E_{xxx}(f_1, f_2) = \delta(f_1-p_1) \delta(f_2-p_1) \delta(f_1+f_2-p_1) \quad (23)$$

This contains the triple product. There will only be a non-zero point in the bispectrum when all three terms in the above product are non-zero. Plotting the three terms in the (f_1, f_2) plane leads to the three lines, $f_1=p_1$, $p_2=p_1$ and $f_1+f_2=p_1$, as shown in Figure 4. For $p_1 \neq 0$ there is no point of intersection of all three lines and hence the bispectrum of a complex sine waves is zero. Next consider a signal consisting of two complex sine waves of frequency p_1 and p_2. The Fourier transform of this signal is,
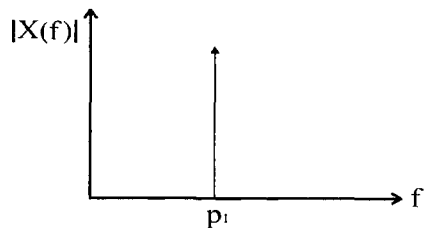

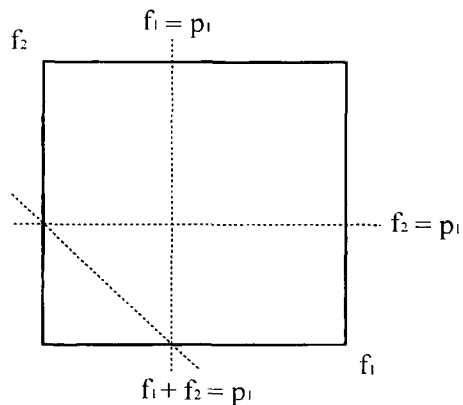**Fig. 3**   Fourier transform of sine wave

Fig. 4   Bispectrum of sine wave

$$X(f) = \delta(f - p_1) + \delta(f - p_2) \qquad (24)$$

This is shown in Figure 5. The deterministic bispectrum is now equal to

$$E_{xxx}(f_1, f_2) = \{ \delta(f_1 - P_1) + \delta(f_1 - p_2) \}$$
$$\{ \delta(f_2 - p_1) + \delta(f_2 - p_2) \} \qquad (25)$$
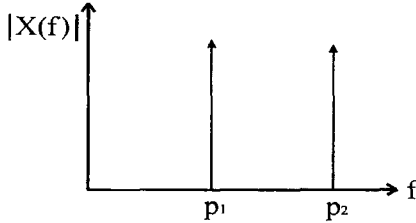$$\{ \delta(f_1 + f_2 - p_1) + \delta(f_1 + f_2 - p_2) \}$$

Fig. 5 Fourier transform of two sine waves $(p_2 = 2 p_1)$
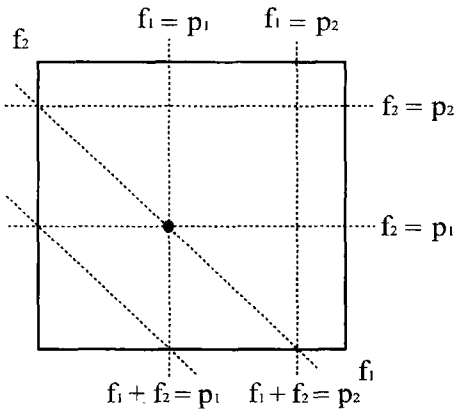
Fig. 6 Bispectrum of two sine waves $(p_2 = 2p_1)$
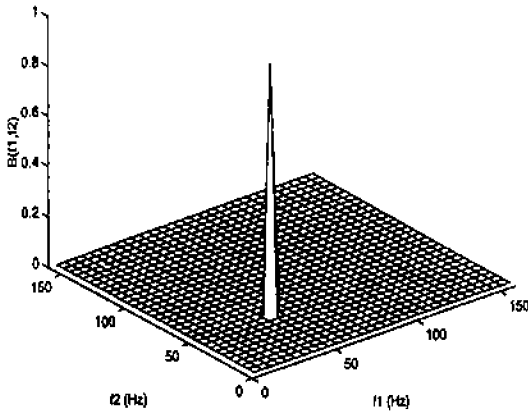
Fig. 7 The bispectrum of two sine waves of frequency 50 Hz and 100 Hz

This can be shown to consist of eight terms, each of which is a triple product. If there are plotted in the (f_1, f_2) plane they appear as the six possible lines $f_1 = p_1$, $f_2 = p_1$, $f_1 = p_2$, $f_2 = p_2$, $f_1 + f_2 = p_1$ and $f_1 + f_2 = p_2$ as shown in Figure 6. There will be an intersection of the three terms if $p_2 = 2p_1$. The Intersection will then occur at (p_1, p_1) as shown by the dot in Figure 6. An example of the bispectrum of two sine waves of frequencies 50 Hz and 100 Hz is shown in Figure 7, where it can be clearly seen that there is a peak at $(50, 50)$ Hz. As the bispectrum is a function of two frequency variables it is easy to plot it as a three dimensional function with the bispectral content rising out of the (f_1, f_2) plane. Here a 'mesh' type plot is used to show the magnitude of the bispectrum as a three dimensional surface. Simple 'contour' maps occasionally allow one to interpret the fine detail with more accuracy as two dimensional surface. The bispectrum is defined as a decomposition of the average of a signal cubed and as such is concerned with the skewness of a signal.

3. Experimental Apparatus and Procedure

Figure 8 shows the experimental apparatus used in the present experiment. The engine used in the experimental work was a 1,500 cc 4-cylinder, 4-stroke unit manufactured by the general automotive company in Korea. The main engine specifications are given in Table 1.

The engine is mounted on a test bed and connected to a HE-130 eddy current dynamometer by a rotor shaft. The exhaust systems are manufactured as shown in Figure 9. Figure 9 shows the experimental test section for pulsating waves in
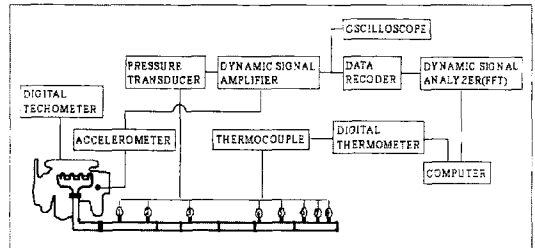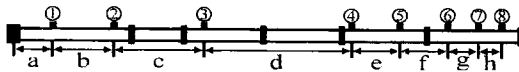

Fig. 8 Schematic diagram of experimental apparatus

Table 2 Specifications for Experimental Engine

| Detail	Description
Displacement, cc	1500
Bore, mm	76.5
Stroke, mm	81.5
Comparison ratio	9.5 : 1
Inlet valve timing (deg)	Open BTDC 18° Close ABDC 57°
Exhaust valve timing (deg)	Open BBDC 60° Close ATDC 13°
Max. Torque (kg·m/rpm)	13.6/3200
Max. Power (ps/rpm)	88/5600

L : 4000 mm, Ø : 40 mm,
a : 210 mm, b : 500 mm, c : 790 mm, d : 1140 mm, e : 450 mm,
f : 450 mm, g : 220 mm, h : 130 mm

Fig. 9   The test section of Exhaust Systems

the exhaust system. The test section is fabricated to divide six parts for the various test condition. The total length of the exhaust system from the valve face to the plain end open to the atmosphere is 4000 mm before bending on chassis body frame of automotive. Engine speed is fixed at 800 rpm, so that the second order harmonic is almost occurred at 50 Hz frequency domain.

At the ①~⑧ points in the exhaust system there are mounted strain-gauge type pressure transducers. The strain-gauge type pressure transducer is fitted to the exhaust pipe by means of water-cooled method. The diaphragm sits flush with the inside wall of the pipe and so avoids the error in pressure indication associated with transducers that have remote diaphragms and connecting indicator passages. The pressure signals are taken at the selected positions along the length of exhaust system for given engine speed and pressure signals are fed to amplifiers. The output from amplifiers is displayed on a Tektronix Type 420 oscilloscope. Figure 10 shows the calibration chart of a pressure transducer used in the experiment. The sensor characteristic is indicated to be linear on the overall pressure range. Also, the accelerometer
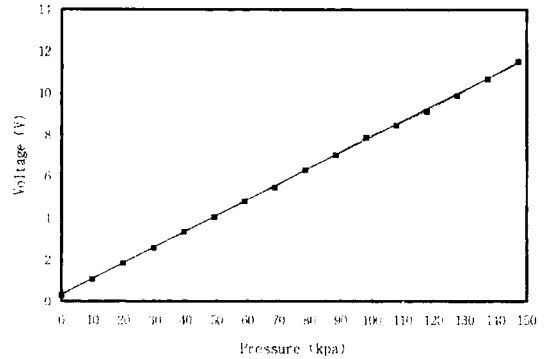
Fig. 10   Pressure transducer calibration chart

for engine excitation measurement is set up engine block of exhaust manifold side. The signal of accelerometer is amplified by amplifier and is displayed on a Tektronix Type 420 oscilloscope. Amplification is controlled that the influence of sensor sensitivity and noise is considered. The signals from the oscilloscope are fed to FFT (Fast Fourier Transformer, HP35670A) and are stored multi-channel data recorder. Power spectrum is obtained on the sampling frequency 500 Hz, the coherence function between inlet signal (③ point) and outlet signal (⑧ point) is obtained. The phase coupling phenomenon of first order fundamental frequency and second order fundamental frequency is expected at ⑥ point. Therefore, bispectrum is obtained at ⑥ point, and the interactions of frequency components are confirmed through bicoherence analysis.

# 4. Experimental Results and Conclusions

The power spectrums of pressure pulsating at measurement point ①~⑧ are given in Figure 11. It is confirmed that the pressure pulsating is consisted of fourth order harmonics. It is observed that the power spectrum value of measurement point ① had the most magnitude at about 25 Hz frequency domain corresponding to ignition frequency of engine speed 800 rpm. The first order harmonic is quickly decreased at measurement point ④. On the other hand, the frequency component magnitude of about 50 Hz frequency domain corresponding to second order harmonic
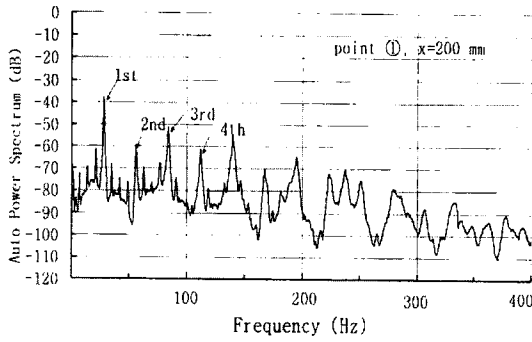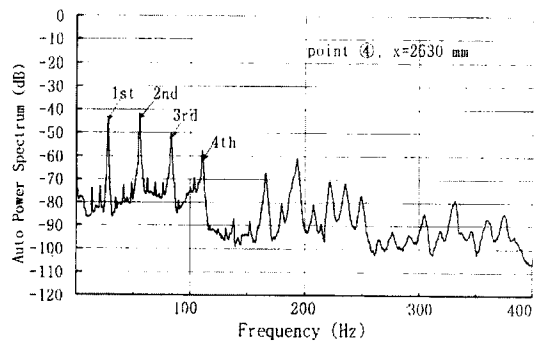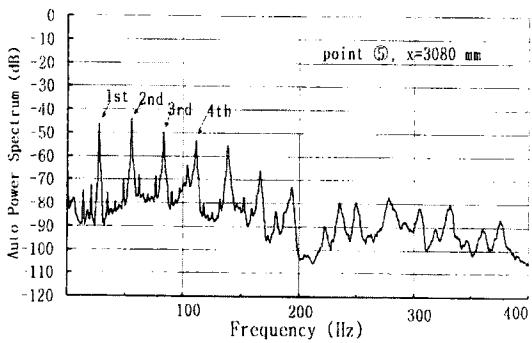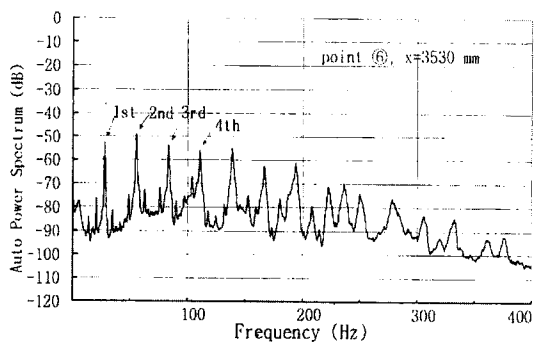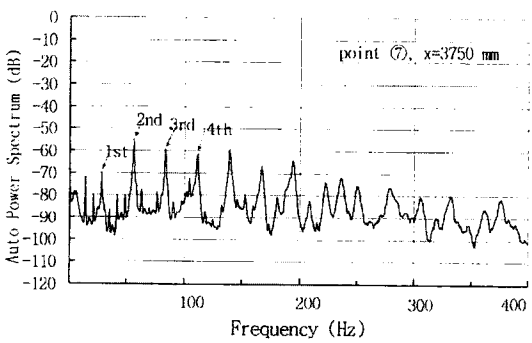
(a) Point 1
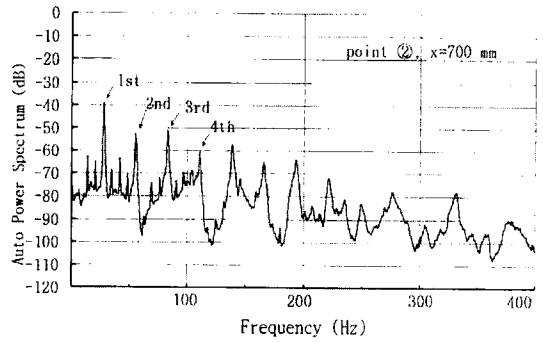
(b) Point 2
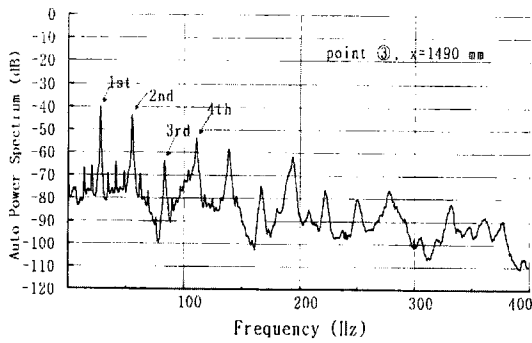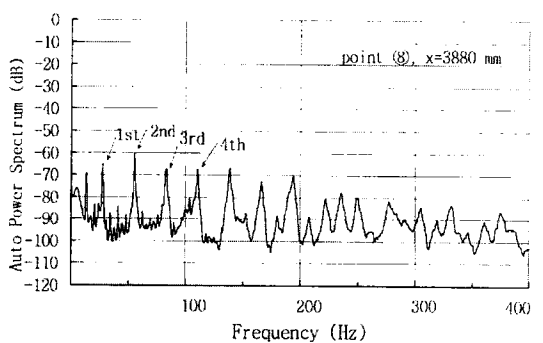
(c) Point 3

(d) Point 4

(e) Point 5

(f) Point 6

(g) Point 7

(h) Point 8

Fig. 11 Power spectrum at each point in exhaust system

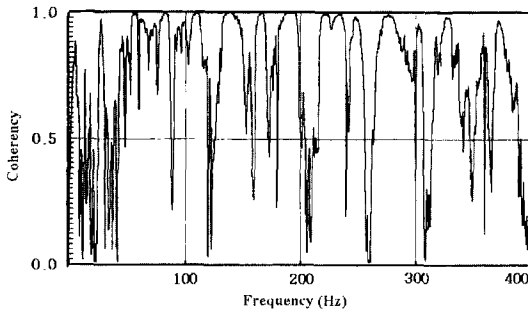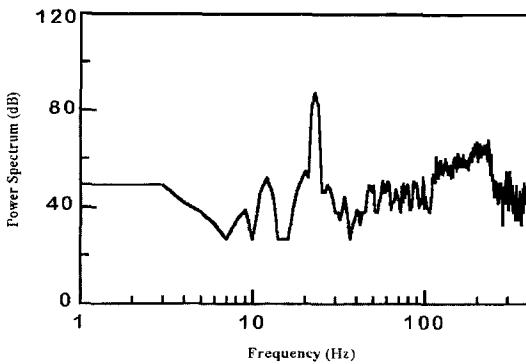**Fig. 12**   Coherence function (between point ③~⑧)

Fig. 13   Power spectrum of engine excitation

Fig. 14   Bicoherence function

$f_1(25$ Hz), $f_2(50$ Hz) and their interactions (f_1+f_2). This is result from the interaction of phase coupling between two waves.

5. Conclusion

is lower than first order component at measurement point ① (at about 20dB degree). But, it is larger than first order component at measurement point ⑥. From the analytical result, the frequency components of pulsating pressure wave are generally decreased, but the second order harmonic of fundamental ignition frequency is nonlinearity grown at specific point. For confirming the properties, the coherence function between inlet signal (③ point) and outlet signal (⑧ point) is indicated in Figure 12. From the coherence function, the lowest frequency 50 Hz is combined another signal. This phenomenon is influenced by excitation of exhaust system about 25 Hz. Figure 13 shows that the power spectrum of engine vibration is excited by engine firing. In Figure 13, engine ignition frequency of about 25 Hz is indicated the most magnitude. The high order spectrum is practiced for confirming the interaction between two waves. Figure 14 shows the bicoherence function. The peak of bicoherence function is indicated at about 25 Hz. It indicates
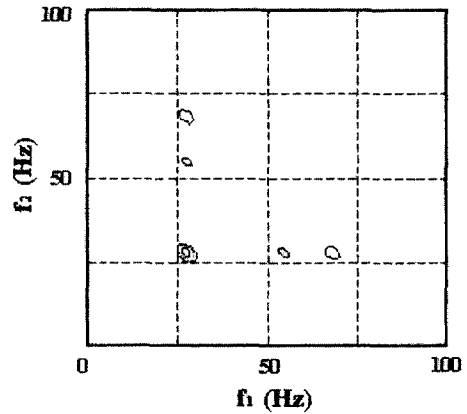
This paper has discussed some of the issues associated with the use of higher order spectra and the application of such techniques to the detection and classification of nonlinearity in automotive exhaust system. The power spectrum, which was only separated to energy density in frequency domain, is not useful to nonlinear phenomenon. Bicoherence can be used to detect the presence of quadratic phase coupling in a signal. Using bicoherence function, formation of second harmonic for interaction of frequency component is confirmed. The bicoherence is normalized bispectra respectively and is predominantly used to measure quadratic phase coupling. Also, bispectrum can be used to detect non-Gaussianity in a signal. If a Gaussian signal is operated on a nonlinear system then the resulting signal will be non-Gaussian. By studying this non-Gaussian signal it is possible to obtain information about possible nonlinearity in the system. In this paper theoretical formulas have been developed to identify the frequency domain properties of two broad types of nonlinear models consisting of finite memory square-law systems that may or may not be in parallel with a separate linear system. The analysis is conducted by using

special bispectral density functions that are function of a single channel instead of the two channels. These special bispectra can be computed by simple extension of procedures currently employed to obtain ordinary spectral density functions. Nonlinear coherence functions, together with ordinary coherence functions, are defined for these nonlinear models using a general methodology for arbitrary nonlinear systems in parallel with arbitrary linear systems.

References

Bendat, J. S. and Piersol, A. G., 1993, "Engineering Applications of Correlation and Spectral Analysis," 2nd Edition, John Wiley & Sons Inc.

Davis, P. O. A. L., 1964, "The Design of Silencers for Internal Combustion Engines," *J. Sound and Vibration*, Vol. 1, No. 2, p. 185.

Eizo Suyama and Takashi Ishida, 1990, "The Optimum Setting Position of the Silencer," *J. SAE*, No. 900348.

Lyon, R. H., 1975, "Statistical Energy Analysis of Dynamical Systems," MIT Press, Cambridge, Massachusetts

Miksad, R. W., Jones, F. L. and Powers, E. J. 1983, "Measurements of Nonlinear Interactions During Natural Transition of a Symmetric Wake," *Physics of Fluids*, Vol. 26, No. 6, pp. 1402~1407.

Mood, A., Graybill, F. A. and Boes, D. C., 1974, "Introduction to the Theory of Statistics," McGraw-Hill.

Nikias, C. L. and Mendel, J. M., 1993, "Signal Processing with Higher-Order Spectra," *IEEE Signal Processing Magazine*, pp. 11~37.

Nikias, C. L. and Petropula, A. P., 1993, "Higher Order Spectra Analysis — A Nonlinear Signal Processing Framework," Prentice Hall.

Nikias, C. L. and Raghuveer, M. R., 1987, "Bispectrum Estimation : A Digital Signal Processing Framework," *Processing of the IEEE*, Vol. 75, No. 7, pp. 869~891.

Priestley, M. B., 1981, "Spectral Analysis and Time Series," Academic Press

Seybert, A. F. and Hamilton, J. F., 1978, "Time delay Bias Errors in Estimating Frequency Response and Coherence Functions," *J. Sound and Vibration*, Vol. 60, No. 1, p. 1.